Full-potential linear muffin-tin-orbital method

K. H. Weyrich*
Max-Planck-Institut für Festkörperforschung, Heisenbergstrasse 1, Postfach 80 06 65, D-7000 Stuttgart 80, Federal Republic of Germany
(Received 14 December 1987)

A new band-structure method which allows the self-consistent solution of the Schrödinger equation with a full (all-electron, non-muffin-tin) crystal potential has been developed. A basis set consisting of the 9 (16) *s*, *p*, and *d* (*f*) linear-muffin-tin orbitals per site is used. The wave functions as well as the electron density and the potential are split into a smooth "pseudo" part, which is expanded in plane waves, and local parts, which are expressed as spherical-harmonics one-center expansions. The total-energy functional of density-functional theory is evaluated without any shape approximation. The usefulness and accuracy of the method is demonstrated by applying it to a "frozen phonon" in silicon and comparing the results with experiment. The calculated phonon frequency and anharmonic term are in excellent agreement with the experimental data. The method is generally applicable to systems with delocalized as well as localized orbitals.

I. INTRODUCTION

In recent years there has been a noticeably growing interest in the first-principles description of solids (for a review, see Ref. 1), i.e., in a description in which the coupling constants of the phenomenological theory are replaced by expressions following from the basic quantum theory of the electron-nucleon system, as discussed, e.g., in Ref. 2. An *ab initio* foundation of lattice dynamics via the "frozen-phonon" concept requires a method which yields accurate total energies or forces. If the Born-Oppenheimer Approximation is accepted and a density-functional (DF) formulation[3] for the many-electron ground-state problem is used, the Hamiltonian describing the dynamics of the nuclei is

$$H=\sum_{\mu}\frac{(\mathbf{P}_{\mu})^2}{2m_{\mu}}+\min_{\{n(\mathbf{r})\}}E[n(\mathbf{r}),\{\mathbf{R}_{\mu}\}]\ , \tag{1.1}$$

where $E[n(\mathbf{r}),\{\mathbf{R}_{\mu}\}]$ is the electronic energy functional, which depends on the electronic density $n(\mathbf{r})$ and the nuclear positions $\mathbf{R}_{\mu}$. Its minimum with respect to $n(\mathbf{r})$ is the ground-state eigenvalue of the many-electron system. $\mathbf{P}_{\mu}$ is the momentum of nucleus μ with mass m_{μ}.

In the Kohn-Sham scheme[4] the minimum of the functional E is found by solving the corresponding Euler-Lagrange equation

$$\left[-\nabla^2+2\int\frac{n(\mathbf{r}')}{|\mathbf{r}-\mathbf{r}'|}d^3r'+v^{\mathrm{xc}}[n,\mathbf{r}]+V^N(\mathbf{r})\right]\psi^j(\mathbf{r})=\varepsilon^j\psi^j(\mathbf{r})\ . \tag{1.2}$$

V^N is the electrostatic potential produced by the nuclei (in atomic Rydberg units).

This Schrödinger-type Kohn-Sham (KS) equation has to be solved self-consistently with the condition

$$n(\mathbf{r})=\sum_{j=1}^{N}|\psi^j(\mathbf{r})|^2\ , \tag{1.3}$$

where the sum runs over the N lowest eigenstates of Eq. (1.2). Density-functional theory (DFT) in the local-density approximation (LDA) yields an explicit expression for the total energy, the Kohn-Sham (KS) functional

$$E[n]=T_s[n]+\int\int\frac{n(\mathbf{r})n(\mathbf{r}')}{|\mathbf{r}-\mathbf{r}'|}d^3r'd^3r+\int\varepsilon^{\mathrm{xc}}(n(\mathbf{r}))n(\mathbf{r})d^3r+\int V^N(\mathbf{r})n(\mathbf{r})d^3r+W^{NN}\ , \tag{1.4}$$

where the exchange-correlation (xc) energy density is connected to the xc potential v^{xc} by

$$v^{\mathrm{xc}}=\frac{\delta}{\delta n}E^{\mathrm{xc}}=n\frac{d\varepsilon^{\mathrm{xc}}}{dn}+\varepsilon^{\mathrm{xc}}\ . \tag{1.5}$$

The ion-ion interaction W^{NN} was added to $E[n]$ in order to obtain the total ground-state energy of the solid.

The application of the theory to lattice statics and dynamics (cohesive properties, equilibrium configurations, phonon frequencies, phase transitions) requires a band-structure method which is suited to yield accurate charge densities and accurate total energies or forces.

A widely used method in electronic-structure calculations is the linear muffin-tin-orbital (LMTO) method,[5,6] which in its simplest solid-state version[7] uses the atomic-sphere approximation (ASA). The LMTO-ASA method is very efficient and yields accurate band structures, lattice constants, and bulk moduli. In contrast to methods like the linear augmented-plane-wave (LAPW) method or methods which use a pure plane-wave basis in connection with a pseudopotential, the LMTO method uses a minimal basis set (9–16 orbitals/sites). Due to the crude approximations (spherically averaged potential and density), the LMTO-ASA method, however, has problems with the calculation of energy variations due to lattice deformations.

In this paper, an LMTO version is developed which, on the one hand, has the advantages of the small LMTO

basis set and its applicability to systems with localized as well as delocalized states and which, on the other hand, avoids spheridizing the potentials and the electron densities in the self-consistency cycle (no shape approximations). The only approximations of our method are therefore those of the finite basis set and the LDA, and we demonstrate that highly accurate "frozen-phonon" frequencies can be obtained. The method is formulated in such a way that the calculations can be performed stepwise in order of increasing complexity and accuracy, starting from ASA—and going to full-potential self-consistency. The technique for evaluating the total energy was developed earlier and applied to various ferroelectrics of the perovskite type.[8,9] In this paper we complete the method by showing how the full potential can be included in the self-consistency cycle without approximations.

In the version developed in this paper, the theory is of an accuracy sufficient for a precise calculation of some of the quantities necessary for a physical understanding, e.g., in the sense discussed in Ref. 2, of unusual phonon properties. Of special interest are such properties which are relevant for a description of structural phase transitions.

The paper is organized as follows. In Sec. II the LMTO Bloch sums are expressed in a way suitable for accurate evaluation of matrix elements and wave functions. These expressions are then used in Sec. III to calculate the Hamiltonian and overlap matrix elements. In Sec. IV the electron density and the resulting Hartree-plus-exchange-correlation potential are determined and, finally, in Sec. V the total energy functional is evaluated. In order to check the accuracy and the usefulness of the method, it was applied to the TO(Γ) phonon of silicon, where experimental information and accurate LAPW and pseudopotential calculations are available. The numerical calculations are reported and discussed in Sec. VI, and Sec. VII gives the summary and conclusions.

II. EXPRESSIONS FOR THE BASIS FUNCTIONS

In the present method linear-muffin-tin orbitals[5,6] (LMTO's) are used as basis functions. They are constructed from a muffin-tin potential $V^{\rm MT}$ which is obtained from a given full potential V by taking the spherical average in spheres around the atomic (or interstitial[10]) sites. In the interstitial region the solid-state LMTO's are solutions of the Laplace equation, i.e., $\nabla^2\chi=0$. The LMTO's are everywhere continuous and differentiable.

The basis orbitals are Bloch sums of LMTO's,

$$\chi_\Lambda^{\mathbf{k}}(\mathbf{r})=\sum_{\mathbf{T}} e^{i\mathbf{k}\cdot\mathbf{T}}\chi_\Lambda(\mathbf{r}-\mathbf{Q}-\mathbf{T}) , \tag{2.1}$$

where Λ ($=\{\mathbf{Q},L\}$) is an abbreviation for the combination of the collective angular momentum index L ($=\{l,m\}$), and the site $\mathbf{Q}$ in the primitive cell. $\mathbf{T}$ are the translation vectors. The Bloch orbitals are split into a smooth "pseudo"-LMTO part $\tilde{\chi}_\Lambda^{\mathbf{k}}$ (Refs. 5 and 11) which extends over the entire space, and a local and strongly varying part which is nonzero only inside the MT spheres and approaches zero continuously and differentiably at the boundaries. The pseudo- and the real LMTO are thus identical in the interstitial region. At the sphere boundaries $\tilde{\chi}$ matches onto χ continuously and differentiably. The smoothness of $\tilde{\chi}$ allows a plane-wave representation

$$\tilde{\chi}_\Lambda^{\mathbf{k}}(\mathbf{r})=\Phi_\Lambda^- \sum_{\mathbf{G}} F_\Lambda(\mathbf{k}+\mathbf{G})e^{i(\mathbf{k}+\mathbf{G})\cdot\mathbf{r}} \tag{2.2}$$

with expansion coefficients of the form

$$F_\Lambda(\mathbf{K})=(2l+1)(2l+3)\frac{4\pi s_{\mathbf{Q}}^3}{\Omega_c}\frac{j_{l+1}(Ks_{\mathbf{Q}})}{(Ks_{\mathbf{Q}})^3} \times Y_L(\hat{\mathbf{K}})e^{-i\mathbf{K}\cdot\mathbf{Q}} . \tag{2.3}$$

Here Ω_c denotes the unit-cell volume and $s_{\mathbf{Q}}$ the radius of the sphere centered at site $\mathbf{Q}$.

The difference between the LMTO and the pseudo-LMTO is a strongly localized function, $\hat{\chi}_\Lambda^{\mathbf{k}}(\mathbf{r})$, which vanishes at and outside spheres and which is everywhere continuous and differentiable. This function is conveniently expressed as the difference between the one-center spherical-harmonics expansions of the LMTO and the pseudo-LMTO inside each sphere. These expansions are[5,6]

$$\chi_\Lambda^{l,\mathbf{k}}(\mathbf{r})=\sum_{\mathbf{T}} e^{i\mathbf{k}\cdot\mathbf{T}}\sum_{\Lambda'}\left[\Phi_{\Lambda'}(\mathbf{r}-\mathbf{Q}-\mathbf{T})\Pi_{\Lambda'\Lambda}^{\mathbf{k}} +\dot{\Phi}_{\Lambda'}(\mathbf{r}-\mathbf{Q}-\mathbf{T})\Omega_{\Lambda'\Lambda}^{\mathbf{k}}\right] , \tag{2.4}$$

$$\tilde{\chi}_\Lambda^{l,\mathbf{k}}(\mathbf{r})=\sum_{\mathbf{T}} e^{i\mathbf{k}\cdot\mathbf{T}}\sum_{\Lambda'}\left[\tilde{\Phi}_{\Lambda'}(\mathbf{r}-\mathbf{Q}-\mathbf{T})\tilde{\Pi}_{\Lambda'\Lambda}^{\mathbf{k}} +\dot{\tilde{\Phi}}_{\Lambda'}(\mathbf{r}-\mathbf{Q}-\mathbf{T})\tilde{\Omega}_{\Lambda'\Lambda}^{\mathbf{k}}\right] , \tag{2.5}$$

where the explicit expressions for the Φ functions and the Π and Ω matrices are given in Refs. 5 and 6 and are summarized in Appendix A. The spherical-harmonics expansions have infinitely many terms, but, since after a particular $l'\equiv l_{\max}$ the centrifugal term dominates the radial Schrödinger equation for $V^{\rm MT}$, we have $\Phi_{l'}(r)=\tilde{\Phi}_{l'}(r)$ and $\dot{\Phi}_{l'}(r)=\dot{\tilde{\Phi}}_{l'}(r)$ for $l'>l_{\max}$ and hence $\Pi_{\Lambda'\Lambda}=\tilde{\Pi}_{\Lambda'\Lambda}$ and $\Omega_{\Lambda'\Lambda}=\tilde{\Omega}_{\Lambda'\Lambda}$, so that the one-center expansion inside any sphere for the difference function,

$$\hat{\chi}_\Lambda^{\mathbf{k}}(\mathbf{r})\equiv\chi_\Lambda^{l,\mathbf{k}}(\mathbf{r})-\tilde{\chi}_\Lambda^{l,\mathbf{k}}(\mathbf{r}) , \tag{2.6}$$

is *finite* and stops at $l_{\max}$.[5] From now on, we shall therefore take the sums over l' in (2.4) and (2.5) to be truncated at $l_{\max}$, and these equations then define the functions $\chi^l(\mathbf{r})$ and $\tilde{\chi}^l(\mathbf{r})$.

In conclusion, we have expressed the LMTO as the sum of a smooth pseudo-LMTO and a remainder which vanishes continuously and differentiably in the interstitial region and whose spherical-harmonics expansion inside any sphere is finite and only has components with $l\le l_{\max}$, viz.,

$$\chi_\Lambda^{\mathbf{k}}(\mathbf{r})=\tilde{\chi}_\Lambda^{\mathbf{k}}(\mathbf{r})+\hat{\chi}_\Lambda^{\mathbf{k}}(\mathbf{r}) . \tag{2.7}$$

These two contributions to the LMTO Bloch sum are sketched in Fig. 1(a). In Fig. 1(b) we show $\tilde{\chi}$ and $\hat{\chi}$, as

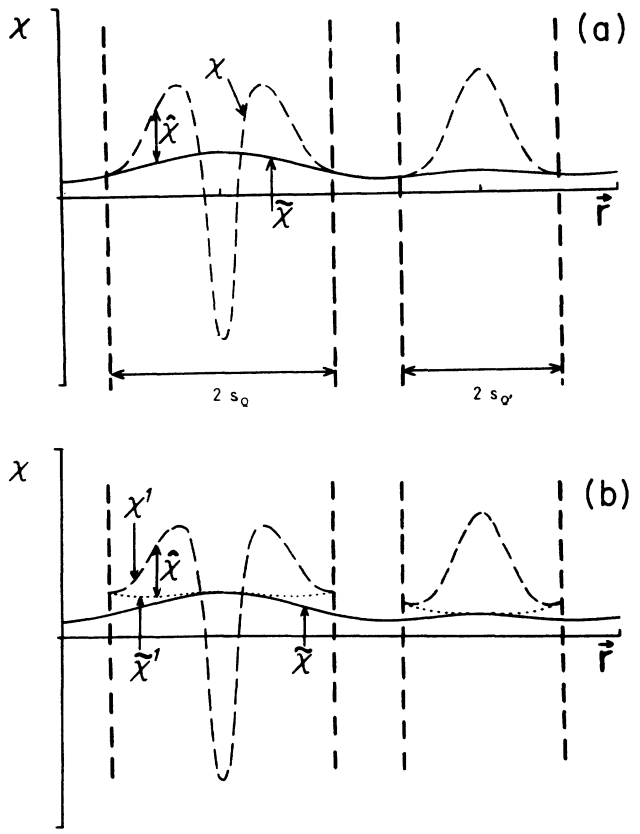

FIG. 1. Schematic plot of a Bloch orbital: (a) pseudoorbital (solid line) and augmentation contribution (dashed line); (b) pseudoorbital (solid line) in comparison to the truncated one-center expansions of the real orbital (dashed line) and the pseudoorbital (dotted line).

well as the two discontinuous contributions, χ^1 and $\tilde{\chi}^1$, to $\hat{\chi}$.

If overlapping Wigner-Seitz (WS) spheres are used instead of MT spheres, a single-valued orbital is obtained by taking the superposition of all $\hat{\chi}$'s that contribute to the overlap region.

The reason for expressing the LMTO Bloch sum in terms of a plane-wave part (2.2) and a local part (2.6) is that the lattice summation (2.1) cannot be performed directly due to the infinite range of the conventional LMTO ($\chi \approx r^{-l-1}$). In the ASA this problem is circumvented by approximating the LMTO Bloch sum by the truncated one-center expansions χ^1 defined in (2.4). The lattice summations can then be performed for the $\underline{\Pi}$ and $\underline{\Omega}$ matrices or, rather, for the structure constants (Appendix A) by use of the Ewald method. The drawback of this procedure is that the one-center expansions converge slowly far away from the centers so that, with $l_{\max}=2$, $\chi^1(\mathbf{r})$ does not go smoothly from one WS sphere to the next. Recently it was shown[12] how the LMTO may be expressed accurately, without the use of a plane-wave expansion but using an exact transformation of the conventional set of LMTO's into a short-ranged, so-called tight-binding set and thereafter performing the direct summation (2.1). This expression has not yet been used to obtain the full potential and the corresponding Hamiltonian matrix.

For comparison with the normal LMTO-ASA expressions for the Hamiltonian and overlap matrices, as well as for the electron density, it is useful to split up the LMTO Bloch sum into the ASA part plus a remainder, i.e.,

$$\chi_\Lambda^{\mathbf{k}}(\mathbf{r})=\chi_\Lambda^{1,\mathbf{k}}(\mathbf{r})+\bar{\chi}_\Lambda^{\mathbf{k}}(\mathbf{r}) . \tag{2.8}$$

The latter,

$$\bar{\chi}_\Lambda^{\mathbf{k}}(\mathbf{r})\equiv\tilde{\chi}_\Lambda^{\mathbf{k}}(\mathbf{r})-\tilde{\chi}_\Lambda^{1,\mathbf{k}}(\mathbf{r}) , \tag{2.9}$$

then equals the LMTO in the interstitial region, is discontinuous at the spheres, and contains merely the high partial waves ($l'>l_{\max}$), whose radial parts are $r^{l'}$, inside the spheres.

In the following sections we shall evaluate matrix elements between LMTO's, as well as the electron density, in a practical way. The basic expression will be the following decomposition of the product of two LMTO Bloch sums:[8]

$$\begin{aligned}\chi_\Lambda^{\mathbf{k}}(\mathbf{r})^*\chi_{\Lambda'}^{\mathbf{k}}(\mathbf{r}')&\equiv|\chi\rangle\langle\chi| \\ &=|\chi^1\rangle\langle\chi^1|+(|\tilde{\chi}\rangle\langle\tilde{\chi}|-|\tilde{\chi}^1\rangle\langle\tilde{\chi}^1|) \\ &\quad+(|\hat{\chi}\rangle\langle\bar{\chi}|+|\bar{\chi}\rangle\langle\hat{\chi}|) ,\end{aligned} \tag{2.10}$$

the correctness of which is easily proved using the definitions (2.6)–(2.9). In expression (2.10) the first term is the "density" in the ASA, and the second term is the difference between the pseudodensity and its ASA; these terms are easily evaluated using (2.2), (2.4), and (2.5). The third term in (2.10) is a correction consisting of the product of the function $\hat{\chi}$, which contains merely low partial waves inside the spheres and which goes smoothly to zero at—and outside—the spheres, and the function $\bar{\chi}$, which contains merely high partial waves inside the spheres, which vanishes like $r^{l_{\max}}$ near the sphere centers, and which is the full LMTO outside the spheres. These two functions are thus orthogonal and hardly overlap so that the third term in (2.10) will give small—or vanishing—contributions.

III. OVERLAP AND HAMILTONIAN MATRICES

The overlap matrix follows from (2.10) by setting $\mathbf{r}=\mathbf{r}'$ and integrating over the cell; as a result

$$\begin{aligned}O^{\mathbf{k}}&\equiv\langle\chi^{\mathbf{k}}|\chi^{\mathbf{k}}\rangle \\ &=\langle\chi^1|\chi^1\rangle+\langle\tilde{\chi}|\tilde{\chi}\rangle-\langle\tilde{\chi}^1|\tilde{\chi}^1\rangle ,\end{aligned} \tag{3.1}$$

since $\langle\hat{\chi}|\bar{\chi}\rangle=0$. On the right-hand side the superscripts $\mathbf{k}$ have been dropped. The first and the last terms in (3.1) are integrals in the spheres and the second term is an integral over the entire cell. Using (2.2)–(2.5) we obtain

$$\begin{aligned}\langle\chi^1|\chi^1\rangle&=\underline{\Pi}^\dagger\underline{\Pi}+\underline{\Omega}^\dagger\underline{P}\,\underline{\Omega} , \\ \langle\tilde{\chi}^1|\tilde{\chi}^1\rangle&=\underline{\tilde{\Pi}}^\dagger\underline{\tilde{\Pi}}+\underline{\tilde{\Omega}}^\dagger\underline{\tilde{P}}\,\underline{\tilde{\Omega}} ,\end{aligned} \tag{3.2}$$

and

$$\langle\tilde{\chi}_\Lambda^{\mathbf{k}}|\tilde{\chi}_{\Lambda'}^{\mathbf{k}}\rangle=\Omega_c\Phi_\Lambda^-\Phi_{\Lambda'}^-\sum_{\mathbf{G}}F_\Lambda^*(\mathbf{k}+\mathbf{G})F_{\Lambda'}(\mathbf{k}+\mathbf{G}) . \tag{3.3}$$

Here, the diagonal matrices $\underline{P}$ and $\underline{\tilde{P}}$ have the elements $\langle \dot{\Phi}_\Lambda^2 \rangle$ and $\langle \dot{\tilde{\Phi}}_\Lambda^2 \rangle$, respectively. This way of evaluating the overlap matrix is conventional and is normally referred to as the ASA plus combined correction.[5]

In order to evaluate the matrix elements of the Hamiltonian we assume that the potential is decomposed into a smooth pseudopart $\tilde{V}$ and a localized part $\hat{V}$ which vanishes continuously and differentiably at—and outside—the spheres:

$$V(\mathbf{r}) \equiv \tilde{V}(\mathbf{r}) + \hat{V}(\mathbf{r}) \ . \tag{3.4}$$

Here

$$\tilde{V}(\mathbf{r}) = \sum_{\mathbf{G}} \tilde{V}(\mathbf{G}) e^{i\mathbf{G}\cdot\mathbf{r}}$$

and

$$\hat{V}(\mathbf{r}) = \sum_{\mathbf{T}} \sum_{\mathbf{Q}} \hat{V}_{\mathbf{Q}}(\mathbf{r}-\mathbf{Q}-\mathbf{T})$$

with

$$\hat{V}_{\mathbf{Q}}(\mathbf{r}) \equiv \sum_{L} \hat{V}_{\mathbf{Q}L}(r) Y_L(\hat{\mathbf{r}}) \ .$$

Each $\hat{V}_{\mathbf{Q}}(\mathbf{r})$ is defined to vanish continuously and differentiably at—and outside—its sphere. Any crystal potential can be expressed in the form (3.4).

The LMTO basis functions are constructed from the MT part of the full potential (3.4). Inside the sphere at $\mathbf{Q}+\mathbf{T}$ this MT potential is

$$V_{\mathbf{Q}}^{\mathrm{MT}}(r) = \tilde{V}_{\mathbf{Q}}^{\mathrm{MT}}(r) + \hat{V}_{\mathbf{Q}}^{\mathrm{MT}}(r) \tag{3.5}$$

with

$$\tilde{V}_{\mathbf{Q}}^{\mathrm{MT}}(r) = \sum_{\mathbf{G}} \tilde{V}(\mathbf{G}) e^{i\mathbf{G}\cdot\mathbf{Q}} j_0(Gr) \Theta(r - s_{\mathbf{Q}}) \tag{3.6a}$$

being the spherical average of the pseudopotential inside the sphere at $\mathbf{Q}$ and

$$\hat{V}_{\mathbf{Q}}^{\mathrm{MT}}(r) \equiv \hat{V}_{\mathbf{Q},\,L=0}(r)/(4\pi)^{1/2} \ . \tag{3.6b}$$

The Hamiltonian matrix elements are now obtained using $-\nabla^2 + V(\mathbf{r})$ together with (2.10). The integrals are over a cell and $-\nabla^2$ is Hermitian between LMTO Bloch sums. Since the latter are everywhere continuous and differentiable we can neglect discontinuities in individual contributions to χ. From the last, small term in (2.10) we therefore obtain $\langle \hat{\chi} | -\nabla^2 | \bar{\chi} \rangle = 0$, because $\bar{\chi}$ is a solution of the Laplace equation, and $\langle \bar{\chi} | -\nabla^2 | \hat{\chi} \rangle = 0$, because $-\nabla^2$ conserves angular momentum. The potential in density-functional theory is a local operator and the last term in (2.10) therefore only picks out the non-MT part, $V - V^{\mathrm{MT}} \equiv V^{\mathrm{NMT}}$, of the potential, i.e., $\langle \hat{\chi} | V | \bar{\chi} \rangle + \mathrm{H.c.} = \langle \hat{\chi} | V^{\mathrm{NMT}} | \bar{\chi} \rangle + \mathrm{H.c}$; this is a very small term. In conclusion, therefore,

$$\begin{aligned}
\underline{H} &\equiv \langle \chi | -\nabla^2 + V | \chi \rangle \\
&= \langle \chi^1 | -\nabla^2 + V | \chi^1 \rangle + \langle \tilde{\chi} | -\nabla^2 + V | \tilde{\chi} \rangle - \langle \tilde{\chi}^1 | -\nabla^2 + V | \tilde{\chi}^1 \rangle + (\langle \hat{\chi} | V^{\mathrm{NMT}} | \bar{\chi} \rangle + \mathrm{H.c.}) \\
&= \langle \chi^1 | -\nabla^2 + V^{\mathrm{MT}} | \chi^1 \rangle && (3.7a) \\
&\quad + \langle \tilde{\chi} | -\nabla^2 | \tilde{\chi} \rangle - \langle \tilde{\chi}^1 | -\nabla^2 | \tilde{\chi}^1 \rangle && (3.7b) \\
&\quad + \langle \tilde{\chi} | \tilde{V} | \tilde{\chi} \rangle - \langle \tilde{\chi}^1 | \tilde{V}^{\mathrm{MT}} | \tilde{\chi}^1 \rangle && (3.7c) \\
&\quad + \langle \chi^1 | V^{\mathrm{NMT}} | \chi^1 \rangle - \langle \tilde{\chi}^1 | \tilde{V}^{\mathrm{NMT}} | \tilde{\chi}^1 \rangle && (3.7d) \\
&\quad + \langle \tilde{\chi} | \hat{V} | \tilde{\chi} \rangle - \langle \tilde{\chi}^1 | \hat{V} | \tilde{\chi}^1 \rangle && (3.7e) \\
&\quad + \langle \hat{\chi} | V^{\mathrm{NMT}} | \bar{\chi} \rangle + \langle \bar{\chi} | V^{\mathrm{NMT}} | \hat{\chi} \rangle \ . && (3.7f)
\end{aligned}$$

The integrals containing χ^1, $\tilde{\chi}^1$, $\hat{\chi}$, V^{MT}, $\tilde{V}^{\mathrm{MT}}$, or $\hat{V}$ only extend inside the spheres.

In the following we discuss the different contributions to the Hamiltonian matrix. The explicit expressions are given in Appendix B in terms of potential parameters and structure constants. Term (a) in Eq. (3.7) is the usual MT or ASA term. The kinetic-energy term (b) vanishes unless the spheres overlap. This is so because $\nabla^2 | \tilde{\chi} \rangle = 0$ in the interstitial region so that if the spheres do not overlap (b) is the sum of the expectation values of $-\nabla^2$ between high partial waves, and the latter are all solutions of the Laplace equation. The terms (c)–(f) are potential-energy terms and describe the influence of the interstitial region and the nonsphericity. The most important term is (c), which contains the complete shape correction and the influence of the nonsphericity of the pseudopotential. Term (d) accounts for the nonspherical part of the potential well inside the spheres. Term (e) is very small because $|\tilde{\chi}\rangle\langle\tilde{\chi}|$ and $|\tilde{\chi}^1\rangle\langle\tilde{\chi}^1|$ give different weightings only in the outer parts of the spheres, and there $\hat{V}$ is small. Similarly, as discussed previously, term (f) is very small. Its evaluation is possible but tedious. Since we have found the influence of the terms (e) and (f) to be vanishingly small in all cases we shall neglect them from now on. The other terms are always included in our calculations, but, at least for Si, the only important effect of the full potential in comparison with the AS or even MT potential comes from term (c).

By expanding the crystal wave function $\psi^{\mathbf{k}j}$ into LMTO's,

$$\psi^{\mathbf{k}j} = \sum_{\Lambda} a_\Lambda^{\mathbf{k}j} \chi_\Lambda^{\mathbf{k}} \ , \tag{3.8}$$

the band structure problem is transformed to the algebraic eigenvalue problem

$$(\underline{H}^{\mathbf{k}}-\varepsilon^{\mathbf{k}j}\underline{O}^{\mathbf{k}})\cdot\underline{a}^{\mathbf{k}j}=0\ . \tag{3.9}$$

The eigenvectors are normalized according to

$$\underline{a}^{\mathbf{k}j\dagger}\cdot\underline{O}^{\mathbf{k}}\cdot\underline{a}^{\mathbf{k}j'}=\delta^{jj'}\ . \tag{3.10}$$

IV. DENSITY AND POTENTIAL

In order to find a self-consistent solution of the KS equations, one has to derive the electron density $n(\mathbf{r})$ from the crystal wave functions $\psi^{\mathbf{k}j}$ and from $n(\mathbf{r})$, the new crystal potential.

According to Eq. (1.2) the *density* is given by the sum of the squares of the wave functions of the occupied states. From Eqs. (2.10) and (3.9) one obtains the valence density

$$n^{v}(\mathbf{r})=2\sum_{\mathbf{k},j}^{\text{occupied}}\sum_{\Lambda,\Lambda'}(a_{\Lambda}^{\mathbf{k}j})^{*}a_{\Lambda'}^{\mathbf{k}j}(\chi_{\Lambda}^{l,\mathbf{k}*}\chi_{\Lambda'}^{l,\mathbf{k}}-\tilde{\chi}_{\Lambda}^{l,\mathbf{k}*}\tilde{\chi}_{\Lambda'}^{l,\mathbf{k}}+\tilde{\chi}_{\Lambda}^{\mathbf{k}*}\tilde{\chi}_{\Lambda'}^{\mathbf{k}})\ . \tag{4.1}$$

Here the cross terms

$$\hat{\chi}^{*}\bar{\chi}+\bar{\chi}^{*}\hat{\chi}$$

are neglected. Inserting Eqs. (2.2), (2.4), and (2.5) into Eq. (4.1) one finds

$$n^{v}(\mathbf{r})=\sum_{\mathbf{T}}\sum_{\mathbf{Q}}\hat{n}_{\mathbf{Q}}^{v}(\mathbf{r}-\mathbf{Q}-\mathbf{T})+\tilde{n}(\mathbf{r}) \tag{4.2}$$

with

$$\hat{n}_{\mathbf{Q}}^{v}(\mathbf{r})=\sum_{L\le 2L_{\max}}\hat{n}_{\mathbf{Q}L}^{v}(r)Y_{L}(\hat{\mathbf{r}}) \tag{4.2a}$$

and

$$\tilde{n}(\mathbf{r})=\sum_{\mathbf{G}}\tilde{n}(\mathbf{G})e^{i\mathbf{G}\cdot\mathbf{r}}\ . \tag{4.2b}$$

The density n^{v} given in Eq. (4.2) thus consists of a localized part $\hat{n}^{v}$ and a pseudopart $\tilde{n}$. $\hat{n}_{\mathbf{Q}}^{v}$ is nonzero only inside the sphere at site $\mathbf{Q}$ and goes continuously and differentiably to zero at the boundary, whereas $\tilde{n}$ is smooth and nonzero everywhere.

One obtains explicitly

$$\hat{n}_{\mathbf{Q}L}^{v}=2\sum_{L',L''}(D_{\mathbf{Q}L'L''}^{\Pi\Pi}\phi_{\mathbf{Q}l'}\phi_{\mathbf{Q}l''}+D_{\mathbf{Q}L'L''}^{\Pi\Omega}\phi_{\mathbf{Q}l'}\dot{\phi}_{\mathbf{Q}l''}+D_{\mathbf{Q}L'L''}^{\Omega\Pi}\dot{\phi}_{\mathbf{Q}l'}\phi_{\mathbf{Q}l''}+D_{\mathbf{Q}L'L''}^{\Omega\Omega}\dot{\phi}_{\mathbf{Q}l'}\dot{\phi}_{\mathbf{Q}l''}$$
$$-D_{\mathbf{Q}L'L''}^{\tilde{\Pi}\tilde{\Pi}}\tilde{\phi}_{\mathbf{Q}l'}\tilde{\phi}_{\mathbf{Q}l''}-D_{\mathbf{Q}L'L''}^{\tilde{\Pi}\tilde{\Omega}}\tilde{\phi}_{\mathbf{Q}l'}\dot{\tilde{\phi}}_{\mathbf{Q}l''}-D_{\mathbf{Q}L'L''}^{\tilde{\Omega}\tilde{\Pi}}\dot{\tilde{\phi}}_{\mathbf{Q}l'}\tilde{\phi}_{\mathbf{Q}l''}-D_{\mathbf{Q}L'L''}^{\tilde{\Omega}\tilde{\Omega}}\dot{\tilde{\phi}}_{\mathbf{Q}l'}\dot{\tilde{\phi}}_{\mathbf{Q}l''})i^{l''-l'}C_{L'L''L} \tag{4.3}$$

with

$$D_{\mathbf{Q}LL'}^{\Pi\Omega}=\sum_{\mathbf{k},j}^{\text{occupied}}\sum_{\bar{\Lambda}\bar{\bar{\Lambda}}}a_{\bar{\Lambda}}^{\mathbf{k},j*}a_{\bar{\bar{\Lambda}}}^{\mathbf{k},j}\Pi_{\bar{\Lambda},\mathbf{Q}L}^{\dagger}\Omega_{\bar{\bar{\Lambda}},\mathbf{Q}L'}$$

and similar expressions for the other $\underline{D}$ matrices. The Gaunt coefficients are

$$C_{LL'L''}=\int Y_{L}^{*}Y_{L'}Y_{L''}^{*}d\Omega$$

and the pseudodensity is

$$\tilde{n}(\mathbf{G})=\sum_{\mathbf{k}}\mathrm{Tr}[\underline{A}^{\mathbf{k}}\cdot\underline{\tilde{S}}^{\mathbf{k}}(\mathbf{G})]$$

with

$$A_{\Lambda\Lambda'}^{\mathbf{k}}=\sum_{j}^{\text{occupied}}a_{\Lambda}^{\mathbf{k}j*}a_{\Lambda'}^{\mathbf{k}j}\Phi_{\Lambda}^{-}\Phi_{\Lambda'}^{-}\ ,$$
$$\tilde{S}_{\Lambda\Lambda'}^{\mathbf{k}}(\mathbf{G})=\sum_{\mathbf{G}'}F_{\Lambda}^{*}(\mathbf{k}+\mathbf{G}')F_{\Lambda'}(\mathbf{k}+\mathbf{G}'+\mathbf{G})\ . \tag{4.4}$$

In practice, the one-center expansion in Eq. (4.2a) is a sum over a few L combinations, which are allowed by the symmetry of the corresponding site. The application of group theory in charge-density calculations with the LMTO method is described in Ref. 13.

The *potential* due to the valence density n^{v} [Eq. (4.2)], the core electron density n^{c}, and the nuclear point charges n^{N} (<0) must now be calculated. The LDA potential consists of a nonlocal Hartree term, produced by all charges in the system and a local xc part, produced by the electrons.

The *Hartree potential* is calculated by solving Poisson's equation for the total charge density ρ. In order that the localized part of the charge density gives rise to localized potential auxiliary charges Δ, which are localized inside, the MT spheres are added and subtracted to the total charge density

$$\rho=(\hat{n}+n^{N}-\Delta)+(\tilde{n}+\Delta)$$
$$=\hat{\rho}+\tilde{\rho}\ . \tag{4.5a}$$

Here we have defined the localized electronic density as

$$\hat{n}=\hat{n}^{v}+n^{c}\ . \tag{4.5b}$$

The Δ's are introduced in order to compensate the multipole moments of the local charge density $\hat{n}+n^{N}$; they have to satisfy the condition

$$\int_{0}^{S_{\mathbf{Q}}}[\hat{n}_{\mathbf{Q}L}^{v}(r)+\sqrt{4\pi}n_{\mathbf{Q}}^{c,N}(r)\delta_{l0}-\Delta_{\mathbf{Q}L}(r)]r^{l+2}dr=0\ . \tag{4.6}$$

If Eq. (4.6) is fulfilled, $\hat{\rho}_{\mathbf{Q}}$ does not produce an electrostatic field outside its own sphere. The influence of the charge in a given sphere on the rest of the crystal is completely described by the field produced by the $\Delta_{\mathbf{Q}}$ which is added to the pseudodensity. Poisson's equation for $\tilde{\rho}$ is solved by Fourier transformation. Therefore, Δ must be smooth enough to ensure a fast convergence of the Fourier series, and the Fourier coefficients should be

known analytically. Our choice is

$$\Delta_{QL}(r)=\begin{cases} d_{QL}r^l\left[1+\cos\frac{\pi}{s_Q}r\right], & r\le s_Q \\ 0 \quad \text{otherwise}, \end{cases} \tag{4.7}$$

which has a discontinuity in the second derivative at the sphere boundary (just as $\tilde{\chi}$). The Fourier coefficients consequently have the asymptotic form

$$\Delta(\mathbf{G})\sim\frac{1}{G^4} \quad \text{as } G\to\infty \ .$$

Explicit expressions for $\Delta(\mathbf{G})$ and d_{QL} are given in Appendix C.

The Hartree potential now arises as a superposition of a localized and a plane-wave part:

$$V^H(\mathbf{r})=\hat{V}^H(\mathbf{r})+\tilde{V}^H(\mathbf{r}) \ , \tag{4.8}$$

where

$$\hat{V}^H(\mathbf{r})=\sum_{\mathbf{T}}\sum_{\mathbf{Q}}\hat{V}^H_{\mathbf{Q}}(\mathbf{r}-\mathbf{Q}-\mathbf{T}) \ ,$$

$$\hat{V}^H_{\mathbf{Q}}(\mathbf{r})=\sum_L \hat{V}^H_{QL}(r)Y_L(\hat{\mathbf{r}}) \ ,$$

$$\hat{V}^H_{QL}(r)=\frac{8\pi}{2l+1}\left[\frac{1}{r^{l+1}}\int_0^r x\hat{\rho}_{QL}(x)dx + r^l\int_r^{s_Q}x^{1-l}\hat{\rho}_{QL}(x)dx\right] ,$$

$$\hat{\rho}_{QL}(x)=\hat{n}^v_{QL}(x)+\sqrt{4\pi}n^{c,N}_{\mathbf{Q}}(x)\delta_{l0}-\Delta_{QL}(x) \ ,$$

and

$$\tilde{V}^H(\mathbf{r})=\sum_{\mathbf{G}}\frac{8\pi}{G^2}[\tilde{n}(\mathbf{G})+\Delta(\mathbf{G})]e^{i\mathbf{G}\cdot\mathbf{r}} \ .$$

In the LDA a smooth density gives rise to a smooth exchange-correlation potential. If we therefore write

$$v^{xc}(n(\mathbf{r}))=\tilde{v}^{xc}(\mathbf{r})+\hat{v}^{xc}(\mathbf{r}) \ , \tag{4.9}$$

then

$$\tilde{v}^{xc}(\mathbf{r})\equiv v^{xc}(\tilde{n}(\mathbf{r})) \tag{4.9a}$$

is smooth, and the remainder

$$\hat{v}^{xc}(\mathbf{r})=v^{xc}(n(\mathbf{r}))-v^{xc}(\tilde{n}(\mathbf{r})) \tag{4.9b}$$

is localized and vanishes continuously and differentiably at—and outside—the spheres. As usual, we now want to express $\hat{v}^{xc}$ as one-center spherical-harmonics series, and $\tilde{v}^{xc}$ as a Fourier series. These series do not, however, follow directly from those for the density because $v^{xc}(n(\mathbf{r}))$ is a nonlinear function of $n(\mathbf{r})$.

We first consider $\hat{v}^{xc}$ and make a Taylor expansion of each term in (4.9b) taking the spherical (MT) part of the respective density (n or $\tilde{n}$) as the large part and the nonspherical (NMT) part as the small part. For the pseudodensity the spherical part is thus

$$\tilde{n}^{MT}_{\mathbf{Q}}(r)=\sum_{\mathbf{G}}\tilde{n}(\mathbf{G})e^{i\mathbf{G}\cdot\mathbf{Q}}j_0(Gr)\Theta(r-s_Q) \tag{4.10a}$$

inside the sphere at $\mathbf{Q}$, and the nonspherical part is

$$\tilde{n}^{NMT}_{\mathbf{Q}}(\mathbf{r})=4\pi\Theta(r-s_Q)\sum_{L>0}i^lY_L(\hat{\mathbf{r}})\sum_{\mathbf{G}}\tilde{n}(\mathbf{G})e^{i\mathbf{G}\cdot\mathbf{Q}}j_l(Gr)Y_L(\hat{\mathbf{G}})^* \ . \tag{4.10b}$$

The spherical and nonspherical parts of the total density to be used in the first term on the right-hand side of (4.9b) are obtained from

$$n^{MT}_{\mathbf{Q}}=\tilde{n}^{MT}_{\mathbf{Q}}+\hat{n}^{MT}_{\mathbf{Q}} \quad \text{and} \quad n^{NMT}_{\mathbf{Q}}=\tilde{n}^{NMT}_{\mathbf{Q}}+\hat{n}^{NMT}_{\mathbf{Q}} \ , \tag{4.10c}$$

where the spherical and nonspherical parts, $\hat{n}^{MT}_{\mathbf{Q}}(r)$ and $\hat{n}^{NMT}_{\mathbf{Q}}(\mathbf{r})$, of the localized valence and core density, $\hat{n}_{\mathbf{Q}}$, follow from (4.2a) and (4.5b). The Taylor expansion thus yields the following spherical-harmonics series for the localized part of the exchange-correlation potential:

$$\hat{v}^{xc}_{\mathbf{Q}}(\mathbf{r})=\sum_L\hat{v}^{xc}_{QL}(r)Y_L(\hat{\mathbf{r}}) \tag{4.11}$$

with

$$\hat{v}^{xc}_{QL=0}(r)/(4\pi)^{1/2}=[v^{xc}(n^{MT})-v^{xc}(\tilde{n}^{MT})] + \frac{1}{4\pi}\left[\frac{1}{2}[v^{xc''}(n^{MT})-v^{xc''}(\tilde{n}^{MT})]\sum_{L'>0}(\tilde{n}_{QL'})^2+\tfrac{1}{2}v^{xc''}(n^{MT})\sum_{L'>0}(\hat{n}^v_{QL'})^2+v^{xc''}(n^{MT})\sum_{L'>0}\hat{n}^v_{QL'}\tilde{n}_{QL'}\right],$$

$$\hat{v}^{xc}_{QL>0}=[v^{xc'}(n^{MT})-v^{xc'}(\tilde{n}^{MT})]\tilde{n}_{QL}+v^{xc'}(n^{MT})\hat{n}^v_{QL} + \sum_{L',L''>0}\{\tfrac{1}{2}[v^{xc''}(n^{MT})-v^{xc''}(\tilde{n}^{MT})]\tilde{n}_{QL'}\tilde{n}_{QL''}+\tfrac{1}{2}v^{xc''}(n^{MT})\hat{n}^v_{QL'}\hat{n}^v_{QL''}+v^{xc''}(n^{MT})\hat{n}^v_{QL'}\tilde{n}_{QL''}\}C_{L'L''L} \ ,$$

where $v^{xc'}$ and $v^{xc''}$ are the first and second derivative of v^{xc} with respect to the density.

In the central parts of the spheres, especially in the core region, the nonsphericity is small as compared to the total density and the Taylor expansion converges rapidly. In the outer region of the sphere, the nonspherical part of the pseudodensity, $\tilde{n}^{NMT}$, is of the same order of magnitude as the total density, but both $\hat{n}^{NMT}$ and the expansion coefficients

$$\left.\frac{d^{(i)}}{dn^{(i)}}v^{xc}(n)\right|_{n=n^{MT}} - \left.\frac{d^{(i)}}{dn^{(i)}}v^{xc}(n)\right|_{n=\tilde{n}^{MT}}, \quad i=0,1,2 ,$$

go continuously and differentiably to zero at the sphere boundary. Thus, the Taylor expansion converges well in the whole sphere.

The pseudopart of the exchange-correlation potential is represented as a Fourier sum. The coefficients

$$\tilde{v}^{xc}(\mathbf{G})=\frac{1}{\Omega_c}\int_{\Omega_c} v^{xc}(\tilde{n}(\mathbf{r}))e^{-i\mathbf{G}\cdot\mathbf{r}}d^3r$$

are determined via a three-dimensional numerical integration over the unit cell. Because of the flatness of $\tilde{n}(\mathbf{r})$ the integration can be performed on a rather wide mesh (e.g., about 4000 grid points in the Si unit cell).

The total crystal potential now has the desired form (3.4). Figure 2 shows our calculated self consistent potential for Si in a (110) plane. The potential is smooth, even at the boundaries of the spheres where the local parts and the pseudoparts match.

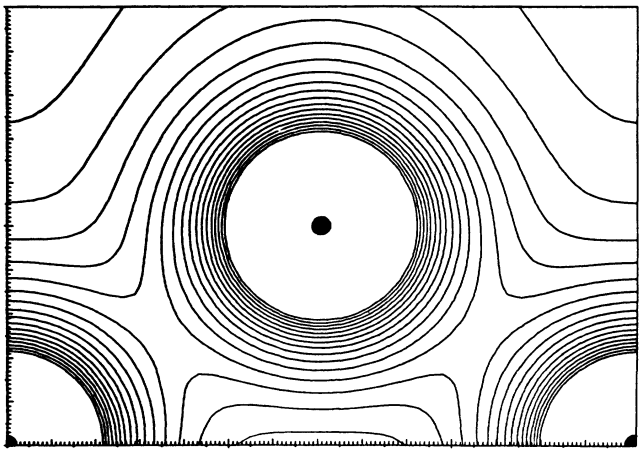

FIG. 2. Self-consistent potential of Si in a (110) plane. The contour interval is 0.25 Ry.

V. TOTAL ENERGY

Density-functional theory gives the total energy $E[n]$ of a many-particle system as a functional of the particle density. We now insert the total charge density ρ given by Eq. (4.5) into $E[n]$, rearrange the terms and subtract the *intra*core interactions, which produce an uninteresting constant when we use the frozen-core approximation, and obtain

$$E[n]=T_s+\hat{E}^{H}+\tilde{E}^{H}+E^{xc}[n]-E^{xc}[n^c] , \tag{5.1}$$

where the kinetic energy, T_s, is calculated by

$$T_s=\sum_{\mathbf{k},j}^{\text{occupied}}\varepsilon^{\mathbf{k},j}-\int_{\Omega_c}V(\mathbf{r})n^{v}(\mathbf{r})d^3r . \tag{5.2}$$

The interaction of the input potential V with the valence density is composed of integrals over spheres and a reciprocal lattice sum. Inserting $V(\mathbf{r})$ given by (3.4) and $n^{v}(\mathbf{r})$ given by Eq. (4.2) one obtains

$$\int_{\Omega_c}V(\mathbf{r})n^{v}(\mathbf{r})d^3r=\Omega_c\sum_{\mathbf{G}}\tilde{V}(\mathbf{G})\tilde{n}^{*}(\mathbf{G})+\sum_{QL}\int_0^{S_Q}[\hat{V}_{QL}(r)\hat{n}^{v}_{QL}(r)+\tilde{V}_{QL}(r)\hat{n}^{v}_{QL}(r)+\hat{V}_{QL}(r)\tilde{n}_{QL}(r)]r^2dr . \tag{5.3}$$

Here $\tilde{V}_{QL}$ and $\tilde{n}_{QL}$ denote the one-center expansion coefficients of $\tilde{V}$ and $\tilde{n}$ in the sphere around site $\mathbf{Q}$:

$$\tilde{V}_{QL}(r)=\sum_{\mathbf{G}}4\pi i^{l}\tilde{V}(\mathbf{G})j_l(Gr)Y_L^{*}(\hat{\mathbf{G}})e^{i\mathbf{G}\cdot\mathbf{Q}} . \tag{5.4}$$

An analogous expression holds for $\tilde{n}_{QL}(r)$.

The intrasphere Coulomb energy has three contributions:

$$\hat{E}^{H}=\sum_{\mathbf{Q}}[\tfrac{1}{2}E^{H}_{\mathbf{Q}}(1)+E^{H}_{\mathbf{Q}}(2)+E^{H}_{\mathbf{Q}}(3)] , \tag{5.5}$$

where each of the terms $E^{H}_{\mathbf{Q}}(i)$ has the form

$$E^{H}_{\mathbf{Q}}(i)=2\sum_{L}\int_0^{S_Q}A^{(i)}_{QL}(r)W^{(i)}_{QL}(r)r^2dr \tag{5.6}$$

with

$$W^{(i)}_{QL}(r)=\frac{8\pi}{2l+1}\left[\frac{1}{r^{l+1}}\int_0^{r}x^{l+2}B^{(i)}_{QL}(x)dx+r^{l}\int_r^{S_Q}x^{1-l}B^{(i)}_{QL}(x)dx\right] \tag{5.7}$$

and

$$\begin{aligned}
A^{(1)}_{QL}&=\hat{n}^{v}_{QL}+\Delta_{QL} ,\\
B^{(1)}_{QL}&=\hat{n}^{v}_{QL}-\Delta_{QL} ,\\
A^{(2)}_{QL}&=\hat{n}^{v}_{QL} ,\\
B^{(2)}_{QL}&=\sqrt{4\pi}n^{c,N}_{\mathbf{Q}}\delta_{l0} ,\\
A^{(3)}_{QL}&=\tilde{n}_{QL} ,\\
B^{(3)}_{QL}&=\hat{n}^{v}_{QL}+\sqrt{4\pi}n^{c,N}_{\mathbf{Q}}\delta_{l0}-\Delta_{QL} .
\end{aligned} \tag{5.8}$$

The *pseudo*-Coulomb energy is

$$\tilde{E}^{H}=4\pi\Omega_c\sum_{\mathbf{G}}\frac{|\tilde{n}(\mathbf{G})+\Delta(\mathbf{G})|^2}{G^2}\ . \tag{5.9}$$

The exchange-correlation energy is treated similarly as the exchange-correlation potential. $E^{xc}[n]$ is split into a cell integral over a smooth function and sphere integrals:

$$E^{xc}[n]=\int_{\Omega_c}\tilde{n}(\mathbf{r})\varepsilon^{xc}(\tilde{n}(\mathbf{r}))d^3r+\hat{E}^{xc}\ . \tag{5.10}$$

The cell integration is done numerically, whereas the integrand of the sphere integrals is expanded in a Taylor series with respect to the nonsphericity n^{NMT}. With

$$v^{xc}(n)=\varepsilon^{xc}(n)+n\frac{d}{dn}\varepsilon^{xc}(n)$$

we obtain, up to second order in n^{NMT}:

$$\hat{E}^{xc}[n]=\sum_{Q}\left\{4\pi\int_0^{S_Q}[n_Q^{MT}\varepsilon^{xc}(n_Q^{MT})-\tilde{n}_Q^{MT}\varepsilon^{xc}(\tilde{n}_Q^{MT})]r^2dr\right.$$
$$\left.+\sum_{L>0}\int_0^{S_Q}\{\tfrac{1}{2}v^{xc'}(n_Q^{MT})(\hat{n}_{QL}^{v})^2+\tfrac{1}{2}[v^{xc'}(n_Q^{MT})-v^{xc'}(\tilde{n}_Q^{MT})](\tilde{n}_{QL})^2+v^{xc'}(n_Q^{MT})\hat{n}_{QL}^{v}\tilde{n}_{QL}\}r^2dr\right\}\ . \tag{5.11}$$

The core xc energy

$$E^{xc}[n^c]=\sum_{Q}4\pi\int_0^{S_Q}n_Q^c\varepsilon^{xc}(n_Q^c)r^2dr$$

is trivial due to the sphericity of n_Q^c.

Notice that the approximations in our total energy expression are consistent with the approximations in the Hamiltonian matrix elements. This ensures that the Schrödinger equation which we solve self-consistently is exactly the Euler-Lagrange equation corresponding to the variational problem

$$\frac{\delta E[n]}{\delta n}=0\ ,$$

and, consequently, the energy behaves variationally in the sense that a small deviation δn from the self-consistent density causes energy deviations of order $(\delta n)^2$.

Even the ASA energy functional (spherical density inside overlapping spheres) is stationary at the self-consistent solution of the ASA Schrödinger equation (spherical potential inside overlapping spheres, calculated from a spherical density). This is the reason why in a self-consistent-field (SCF) run the ASA total energy converges much faster than the ASA potential and the ASA band energies. Nevertheless, the ASA energy functional is not the HK energy functional for a given (spherical) density.[14]

In contrast to the ASA, the total energy expression derived above is the HK energy evaluated for a given density, but due to the limited basis set ($L_{max}<\infty$, $\kappa^2=0$) the obtainable densities are confined to a certain subspace.

Up until now, the method was formulated with strictly MT (i.e., not overlapping) spheres. If the spheres are blown up to overlapping atomic spheres, the basis orbitals [Eq. (2.7)] and the density [Eq. (4.2)] are still well-defined single-valued functions, continuous, and differentiable. But the expression derived for the total energy [Eq. (5.1)] becomes inaccurate due to a wrong treatment of the overlap region. The Hartree energy is wrong by

$$\int\int\frac{\hat{n}_Q(\mathbf{r})\hat{n}_{Q'}(\mathbf{r}')}{|\mathbf{r}-\mathbf{r}'|}d^3r'\,d^3r$$

where the integral runs over the overlap region.

Similar terms are missing in the kinetic and exchange-correlation energy. Since $\hat{n}$ is small in the overlap region ($\hat{n}$ approaches zero continuously and differentiably) these energy corrections are small. In frozen-phonon calculations, however, where the result depends on energy differences of the order of 0.1 mRy, these terms become important.

In practice the evaluation of $E[n]$ is simplified by replacing the sphere integrals

$$\int_0^{S_Q}\tilde{n}_{QL}\hat{V}_{QL}r^2dr\ \text{ and }\ \int_0^{S_Q}\tilde{n}_{QL}W_{QL}^{(3)}r^2dr \tag{5.12}$$

by

$$\int_0^{S_Q}\tilde{n}_{QL}^{1}\hat{V}_{QL}r^2dr\ \text{ and }\ \int_0^{S_Q}\tilde{n}_{QL}^{1}W_{QL}^{(3)}r^2dr\ , \tag{5.13}$$

where $\tilde{n}_{QL}^{1}$ is the density obtained by the one-center expansion $\tilde{\chi}^1$ [see Eqs. (4.1) and (4.3)]. The difference between $\tilde{n}_{QL}$ and $\tilde{n}_{QL}^{1}$ is relevant close to the boundary of the sphere, but there the potentials $\hat{V}_{QL}$ and W_{QL}^{3} become small by construction. On the other hand, these potentials are very large close to the center of the spheres, and small errors in $\tilde{n}$, due to an incomplete convergence of the Fourier series, lead to noticeable changes in the result. The above replacement therefore diminishes the cutoff dependence of the total energy.

VI. NUMERICAL TEST OF THE METHOD

In this section the method is applied to silicon, where experimental as well as accurate theoretical (LAPW,[15] pseudopotential,[16–18] and multiple Green's function[19]) results are available for comparison. Several approximations and their influence on the electron density, the cohesive energy, and the phonon frequencies will be discussed.

The only (essential) approximation in the presented LMTO version is the restriction to zero kinetic energy in the interstitial region ($\kappa^2=0$). This limitation causes an

incompleteness of the basis set in the interstitial region. In ASA the interstitial region is eliminated by enlarging the MT spheres to space filling WS spheres. In our method, the size of the spheres may still be chosen, and we discuss the accuracy of the results as a function of the radii.

There are three quantities of interest which are given by an electronic ground-state calculation: the band structure (band energies, density of states), the electron density, and the total energy. Their variation, due to a phonon distortion, is of special interest. It yields the deformation potentials, the deformation densities, and the phonon frequencies, respectively.

A. Application to cubic Si

Our self-consistent calculations are performed in the frozen-core approximation. The core density was determined by a relativistic free-atom calculation. The $3s$ and $3p$ electrons are included in the scalar relativistic band calculation. For the local exchange-correlation potential we use the parametrization by von Barth and Hedin.[20] Empty spheres, which have the same size as the Si spheres, are fitted into the diamond structure to obtain a bcc structure. The integrations over the irreducible part of the fcc Brillouin zone are replaced by weighted summations over the two special points[21]

$$\mathbf{k}^1=\frac{2\pi}{a}(\tfrac{3}{2},\tfrac{1}{4},\tfrac{1}{4}) \quad \text{and} \quad \mathbf{k}^2=\frac{2\pi}{a}(\tfrac{1}{4},\tfrac{1}{4},\tfrac{1}{4})$$

with weights

$$\alpha^1=\frac{3}{4} \quad \text{and} \quad \alpha^2=\tfrac{1}{4}\ .$$

Previously, it was shown that accurate *band energies* are obtained in ASA if empty spheres are placed to the empty sites of the diamond structure and the "combined correction term" (CCT) is included.[10] This was confirmed by our calculations. The full potential is not necessary if WS spheres are used, whereas the inclusion of the nonsphericity of the potential brings a substantial improvement as compared to the spherical potential if MT spheres are used.

The same trend is recognizable if the influence of different approximations on the *charge density* $n(\mathbf{r})$ is investigated. Figure 3 shows a contour plot of the calculated density in the Si (110) plane in comparison with the x-ray-determined electron density[22] (same contour values in both plots). The calculation gives practically the same result (with irrelevant differences) for the spherical WS-potential (WSP) and the full potential (FP) if WS spheres are used as augmentation spheres for the orbitals (WSO). This was demonstrated in Ref. 12. On the other hand, if MT augmentation spheres are used it is necessary to perform a full potential calculation (FP-MTO) in order to obtain a satisfactory charge density. A spherical average of the potential in the MT spheres changes the density drastically (MTP-MTO). This is demonstrated in Fig. 4. The results of the FP-MTO and the FP-WSO calculations are nearly identical and both agree quite well with the experimental result (see Fig. 3).

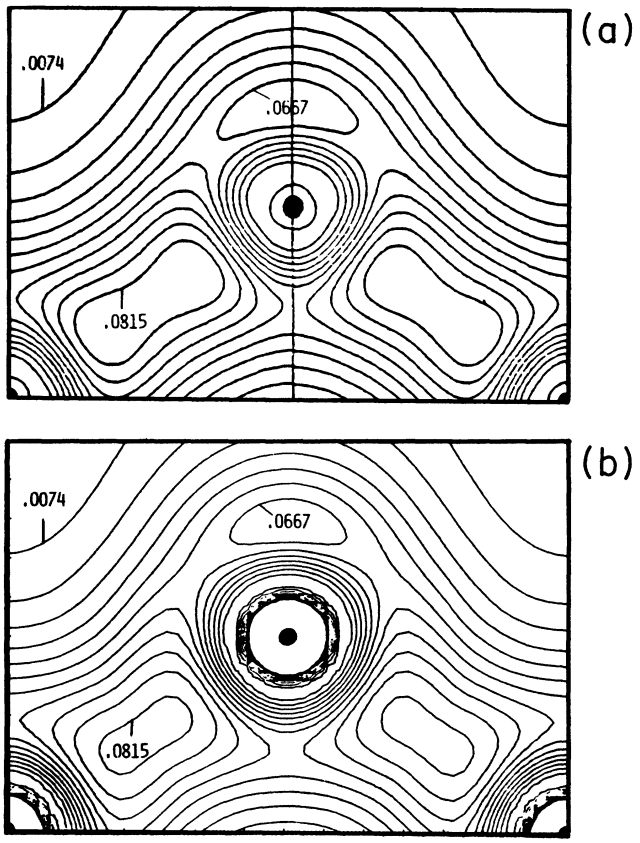

FIG. 3. (a) Measured electron density of Si in the (110) plane (Ref. 22), in comparison to (b) the calculated (FP-WSO) density. The contour values are given in electrons/bohr^3, the contour interval is 0.0074 electrons/bohr^3 (same contour values in both parts). The experimental density was measured with different x-ray sources (left part, Mo; right part, Ag).

Next we consider the *cohesive energy*, which is the difference between the crystal total energy and the total energy of the isolated atoms. In DFT the best electron density gives the lowest total energy, which means that the cohesive energy is a measure for the accuracy of the calculated charge density, provided the KS functional $E[n]$ is evaluated exactly for a given density.

The cohesive energy in the LDA and ASA is -5.0 eV/atom,[23] whereas other methods, without shape approximation, give values between -5.3 and -5.4 eV/atom.[17,19] The main defect of the ASA is the spherical average of the density. If we do not use this approximation but keep the potential spherical inside WS spheres (WSP-WSO),[12] the result changes to about -5.35 eV/atom. The inclusion of the nonsphericity of the potential causes a further lowering of E_{coh} by about 0.01 eV/atom. This result is in agreement with the fact that $n(\mathbf{r})$ calculated from an ASA potential is close to the full potential $n(\mathbf{r})$. If we change the spheres to MT spheres, E_{coh} increases to -4.75 eV/atom, which reflects the incompleteness of the basis set in the interstitial region.

Unfortunately, E_{coh} calculated with the nonspherical density converges very slowly as a function of the

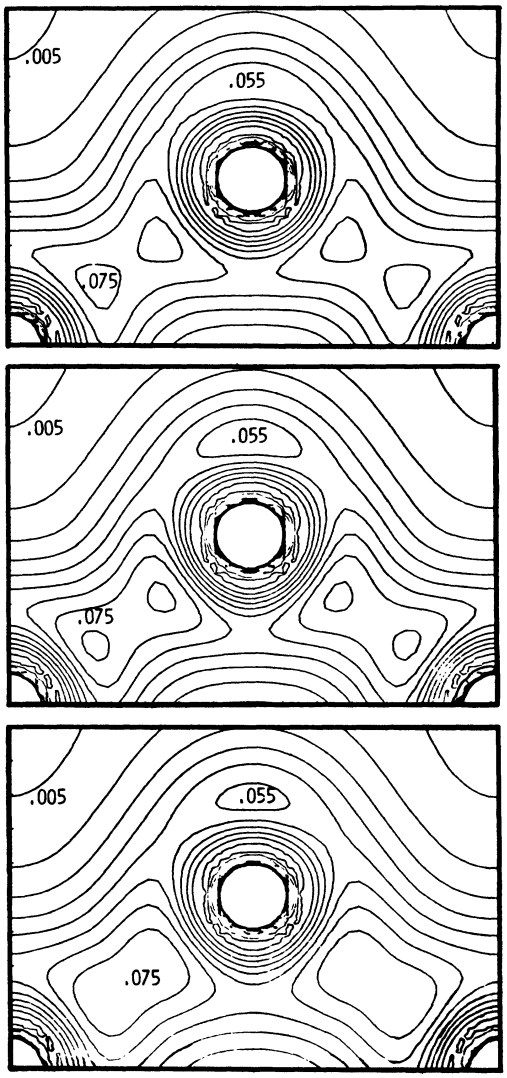

FIG. 4. Comparison of electron densities in Si calculated with different approximations: (a) muffin-tin potential, muffin-tin augmentation spheres (MTP-MTO); (b) full-potential, muffin-tin augmentation spheres (FP-MTO); (c) full-potential, Wigner-Seitz augmentation spheres (FP-WSO). The contour values are given in electrons/bohr^3, the contour interval is 0.005 electrons/bohr^3.

Fourier-expansion cutoff, $G_{\max}$, of the pseudo-wavefunctions. In order to obtain variations of E_{coh} less than ± 0.07 eV/atom, $G_{\max}$ must be larger than $9(2\pi/a)$. This strong dependence of E_{coh} on $G_{\max}$ is due to variations in the interactions of the pseudodensity with the strong core potential. It is reduced if $\tilde{n}$ is replaced by $\tilde{n}^{1}$ [which is independent of $G_{\max}$, see Eqs. (5.12) and (5.13)] in these terms and the convergence is better than 0.02 eV/atom for $G_{\max} \gtrsim 6(2\pi/a)$.

In the above expression for $E[n]$ the cutoff $G_{\max}$ is not a variational parameter (in contrast to the situation for LAPW and pseudopotential calculations). Consequently, the G sums have to be convergent in order to obtain a total energy which behaves variationally with respect to a variation of the input potential or of the basis set.

B. Frozen phonon in Si

In recent years, first-principles calculations of phonon frequencies and structural energy differences have been of great interest. A well investigated example is the optical Γ-point phonon of Si, which has the interesting feature of a strong anharmonicity. The phonon is threefold degenerate and we choose the polarization vector in such a way that it describes the displacement of one of the two Si atoms in the unit cell in the 111 direction. The two position vectors are in units of the lattice constant a

$$\mathbf{Q}^1=(0,0,0), \quad \mathbf{Q}^2=(1+\gamma)(\tfrac{1}{4},\tfrac{1}{4},\tfrac{1}{4}) ,$$

where γ is the amplitude of the phonon. In addition to the two Si atoms there are two empty (E) spheres per unit cell. In the undistorted crystal, the two Si spheres are followed by two E spheres along the 111 direction, with equal distances between all neighboring spheres. In the distorted crystal, the positions of the E spheres are no longer fixed by symmetry. We studied two cases.

Case I:

$$\begin{aligned} \mathbf{Q}^3&=(2+\gamma)(\tfrac{1}{4},\tfrac{1}{4},\tfrac{1}{4}) , \\ \mathbf{Q}^4&=3(\tfrac{1}{4},\tfrac{1}{4},\tfrac{1}{4}) . \end{aligned} \tag{6.1a}$$

Case II:

$$\begin{aligned} \mathbf{Q}^3&=\left[2+\frac{\gamma}{2}\right](\tfrac{1}{4},\tfrac{1}{4},\tfrac{1}{4}) , \\ \mathbf{Q}^4&=\left[3+\frac{\gamma}{2}\right](\tfrac{1}{4},\tfrac{1}{4},\tfrac{1}{4}) . \end{aligned} \tag{6.1b}$$

Because of the symmetry breaking by the phonon, the $\mathbf{k}$ integration has now to be performed over the rhombohedral irreducible Brillouin zone. The integration is replaced by a summation over five special points $\mathbf{k}^i$ with weights α^i:

$$\mathbf{k}^1=\frac{2\pi}{a}\frac{1}{4}(1,1,1), \quad \alpha^1=\tfrac{1}{16} ,$$

$$\mathbf{k}^2=\frac{2\pi}{a}\frac{1}{4}(-1,1,-1), \quad \alpha^2=\tfrac{3}{16} ,$$

$$\mathbf{k}^3=\frac{2\pi}{a}\frac{1}{4}(1,3,1), \quad \alpha^3=\tfrac{3}{16} ,$$

$$\mathbf{k}^4=\frac{2\pi}{a}\frac{1}{4}(3,1,-1), \quad \alpha^4=\tfrac{3}{8} ,$$

$$\mathbf{k}^5=\frac{2\pi}{a}\frac{1}{4}(3,-1,-1), \quad \alpha^5=\tfrac{3}{16} .$$

The variation of the total energy

$$\Delta E(\gamma)=E(\gamma)-E(\gamma=0)$$

as a function of the distortion γ for a shift of the empty spheres according to case I is shown in Fig. 5, for various approximations, in comparison to the experimental curve [determined from phonon frequency and third-order elastic force constants (see Ref. 16)]. Pure ASA (potential spherical, density spherical) yields an unphysical result: the crystal is unstable against the phonon distortion (□ in Fig. 5). A substantial improvement is obtained if the den-

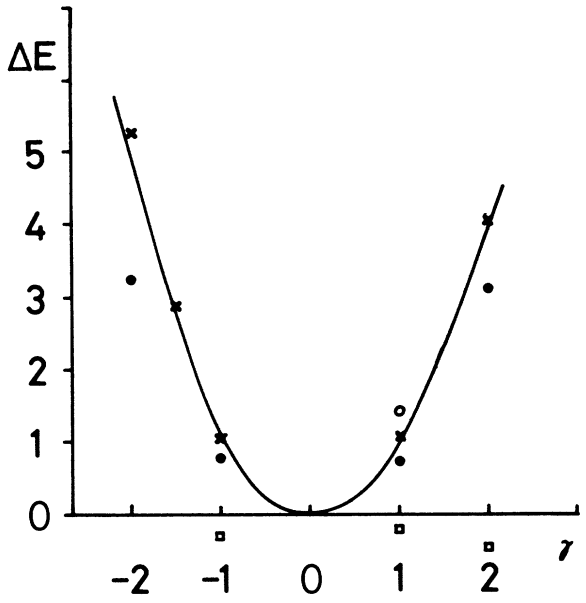

FIG. 5. Total energy variation (in mRy) as a function of the phonon amplitude given in units of $0.005\sqrt{3}a$ (a is the lattice constant) for various approximations, in comparison to the experimental result (solid line) (see Ref. 16). ×: Full-potential LMTO, MT augmentation spheres (FP-MTO). ●: Rigid ASA potential, nonspherical density, WS augmentation spheres (WSP-WSO). ○: Rigid muffin-tin potential, nonspherical density, MT augmentation spheres (MTP-MTO). □: Rigid ASA potential, ASA density.

sity is not spheridized any more but the potential used to determine the density is still the result of a self-consistent ASA calculation (WSP-WSO). The square of the frequency has the correct sign but the calculated energy differences (● in Fig. 5) and frequencies are still too low as compared to the experimental values (solid curve in Fig. 5 for ΔE) by about 30% and 15%, respectively. In all these calculations, the potential was the self-consistent ASA potential obtained for $\gamma=0$ and was shifted rigidly under the distortion ($\gamma\neq 0$). ASA self-consistency for $\gamma\neq 0$ would flatten the energy parabola even further. Going to self-consistency in the full potential but keeping the augmentation spheres as overlapping WS spheres does not improve the results (FP-WSO). On the other hand, if instead of a rigid WS-potential a rigid MT-potential (MTP-MTO) is used, the energy variation is overestimated (○ in Fig. 5). Excellent agreement with the experimental values is obtained from a full-potential calculation (× in Fig. 5) with spheres which are so small that they do not overlap even in the distorted crystal (FP-MTO). The frequency and the anharmonicity are described well. The results of FP-MTO calculations are almost independent of the position of the empty spheres: If the empty spheres are shifted from the positions of case I to that of case II [cf. Eq. (6.1)], the energy difference is about 0.02 mRy. In addition, the calculated $\Delta E(\gamma)$ is essentially independent of the cutoff $G_{\max}$ if $G_{\max} \gtrsim 5(2\pi/a)$.

These results show that a frozen-phonon calculation is sensitive to errors in $E[n]$: An inaccurate treatment of the overlap region, which occurs if WS augmentation spheres are used, leads to an error of 15% in the calculated frequency.

VII. SUMMARY AND CONCLUSIONS

A new full-potential band-structure method based on the linear muffin-tin-orbital (LMTO) method was developed. In connection with density-functional theory in the local-density approximation it allows total-energy calculations which are sufficiently accurate for "frozen-phonon" calculations. A minimal basis set of 9–16 LMTO's per site is used. For neither the potential nor the density is a shape approximation used. Muffin-tin or Wigner-Seitz spheres are needed only as augmentation spheres for the definition of the basis orbitals. The variational principle allows the optimization of the radii by minimalization of the total energy with respect to the radii.[24] There are some similarities between the LMTO method presented above and the full-potential linear augmented-plane-wave (LAPW) method.[5,25,26] Roughly speaking, the LAPW's are linearly combined to the smaller set of LMTO's with zero kinetic energy ($\kappa^2=0$) in the interstitial region. The incompleteness of the basis set in the interstitial region has some influence on the cohesive energy but not on the phonon frequencies. In an open structure, the volume of the interstitial region is reduced by inserting empty spheres into the open regions of the crystal. Small displacements of the empty spheres have no influence on the total energy.

The application to silicon yielded information about the influence of several approximations. In spite of the use of spherically averaged potentials, the atomic-sphere approximation produces a charge density which is very close to the experimental one and is much better than that calculated from a muffin-tin potential. The energy variation due to a phonon distortion, as obtained from a spherical potential, however, is only in qualitative agreement with a full-potential calculation. These investigations have shown that an accurate "frozen-phonon" calculation requires a full-potential method.

Recently, our method was applied to the group-IV semiconductors and to some III-V compounds.[27] In all cases, the calculated phonon frequencies are in excellent agreement with experiment. An application to the more complex systems of perovskite-type ferroelectrics showed the general applicability of the method.[28] The lattice instability of $BaTiO_3$ with respect to the ferroelectric TO(Γ) mode was found. The method presented in this paper allows, thus, for deformed, relatively complex compounds first-principles calculations which are of an accuracy sufficient for a discussion of, e.g., sequences of structural phase transitions.

ACKNOWLEDGMENTS

The author is grateful to O. K. Anderson for supplying many of the basic ideas and to O. Jepsen, M. S. Methfessel, P. Blöchl, N. E. Christensen, and R. Siems for helpful discussions. This work was partially supported by the Deutsche Forschungsgemeinschaft (Bonn, Germany) within Sonderforschungsbereich "Ferroelektrika."

APPENDIX A: WAVE FUNCTIONS AND POTENTIAL PARAMETERS

A basis orbital $\chi_{QL}(\mathbf{r}-\mathbf{Q}-\mathbf{T})$ centered at a position $\mathbf{Q}$ in the unit cell at $\mathbf{T}$ with angular momentum $L=(l,m)$ is obtained from a multiple field

$$K_{TQL}(\mathbf{r})=\left[\frac{x}{\bar{s}}\right]^{-l-1} i^l Y_L(\hat{\mathbf{x}}),\quad \mathbf{x}=\mathbf{r}-\mathbf{Q}-\mathbf{T} \tag{A1}$$

by $\phi,\dot{\phi}$ augmentation. Here $\bar{s}$ denotes the average radius of space-filling spheres. Inside the sphere at $\mathbf{T}+\mathbf{Q}$, the radial part of K is replaced by

$$\Phi_{Ql}(-l-1,r)=\phi_{Ql}(r)+\omega_{Ql}^{-}\dot{\phi}_{Ql}(r)\ , \tag{A2}$$

whose logarithmic derivative at the boundary is $-l-1$. Inside the sphere at $\mathbf{T}'+\mathbf{Q}'$ the one-center expansion of the multipole field is

$$K_{TQL}(\mathbf{r})=-\sum_{L'=0}^{\infty}\frac{1}{2(2l'+1)}\left[\frac{x'}{\bar{s}}\right]^{l'} i^{l'}Y_{L'}(\hat{\mathbf{x}}')S_{T'Q'L',TQL}\ , \tag{A3}$$

$$\mathbf{x}'=\mathbf{r}-\mathbf{Q}'-\mathbf{T}'$$

and the radial functions are replaced by

$$\Phi_{Ql}(l,r)=\phi_{Ql}(r)+\omega_{Ql}^{+}\dot{\phi}_{Ql}(r) \tag{A4}$$

with a logarithmic derivative l' at the boundary. The function ϕ_{Ql} is the solution of the radial Schrödinger equation inside the sphere $\mathbf{Q}$ with energy E_{Ql} and $\dot{\phi}_{Ql}$ is its energy derivative.

The matrices $\Pi^{\mathbf{k}}$ and $\Omega^{\mathbf{k}}$ appearing in the one-center expansion of the Bloch sum, Eq. (2.4), are

$$\Pi^{\mathbf{k}}_{\Lambda\Lambda'}=\delta_{\Lambda\Lambda'}-(\phi^{+}_{\Lambda})^{-1}S^{\mathbf{k}}_{\Lambda\Lambda'}\phi^{-}_{\Lambda'} \tag{A5}$$

and

$$\Omega^{\mathbf{k}}_{\Lambda\Lambda'}=\omega^{-}_{\Lambda}\delta_{\Lambda\Lambda'}-\omega^{+}_{\Lambda}(\phi^{+}_{\Lambda})^{-1}S^{\mathbf{k}}_{\Lambda\Lambda'}\phi^{-}_{\Lambda'}\ ,$$

where

$$S^{\mathbf{k}}_{\Lambda\Lambda'}=\sum_{\mathbf{T}} e^{i\mathbf{k}\cdot\mathbf{T}}S_{TQL,T'Q'L'}$$

are the usual Fourier-transformed LMTO structure constants.[5,6]

The potential parameters ϕ^{-} and ϕ^{+} are obtained from the wave functions at the boundaries of the sphere,

$$\Phi^{-}_{\Lambda}=\Phi_{\Lambda}(-l-1,s_Q)\ , \tag{A6}$$
$$\Phi^{+}_{\Lambda}=\Phi_{\Lambda}(l,s_Q)\ ,$$

by

$$\phi^{-}_{\Lambda}=\left[\frac{\bar{s}}{s_Q}\right]^{-l-1}\left[\frac{\bar{s}}{2}\right]^{1/2}\Phi^{-}_{\Lambda}\ ,$$
$$\phi^{+}_{\Lambda}=2(2l+1)\left[\frac{\bar{s}}{s_Q}\right]^{l}\left[\frac{\bar{s}}{2}\right]^{1/2}\Phi^{+}_{\Lambda}\ . \tag{A7}$$

The "pseudo"-wave functions as well as the potential parameters are known analytically:[5]

$$\tilde{\phi}_{Ql}(r)=\left[\frac{2l+3}{(s_Q)^3}\right]^{1/2}\left[\frac{r}{s_Q}\right]^{l},$$

$$\dot{\tilde{\phi}}_{Ql}(r)=\tfrac{1}{2}[(2l+3)s_Q]^{1/2}\left[\frac{1}{2l+5}\left[\frac{r}{s_Q}\right]^{l}-\frac{1}{2l+3}\left[\frac{r}{s_Q}\right]^{l+2}\right],$$

$$\tilde{\phi}^{-}_{Ql}=\left[\frac{s_Q}{\bar{s}}\right]^{l+1/2}\frac{2l+5}{[8(2l+3)]^{1/2}s_Q}\ ,$$

$$\tilde{\phi}^{+}_{Ql}=\left[\frac{\bar{s}}{s_Q}\right]^{l+1/2}\frac{2l+1}{s_Q}\left[\frac{2}{2l+3}\right]^{1/2},$$

$$\tilde{\omega}^{-}_{Ql}=\frac{(2l+1)(2l+5)}{2(s_Q)^2}\ ,$$

$$\tilde{\omega}^{+}_{Ql}=0\ ,$$

$$\langle\dot{\tilde{\phi}}^{2}_{Ql}\rangle=\int_0^{s_Q}\dot{\tilde{\phi}}^{2}_{Ql}(r)r^2dr=\frac{(s_Q)^4}{(2l+3)(2l+5)^2(2l+7)}\ .$$

The one-center expansion coefficients of Eq. (2.5) are obtained from Eq. (A5) by replacing the real-potential parameters by the pseudopotential parameters.

APPENDIX B: HAMILTONIAN MATRIX ELEMENTS

The derivation of explicit expressions for the Hamiltonian matrix contributions (a)–(d) of Eq. (3.7) is straightforward.

Term (a), the usual MT term, is obtained by inserting Eq. (2.4) into Eq. (3.7a):

$$\langle\chi^1\,|\,-\nabla^2+V^{\mathrm{MT}}\,|\,\chi^1\rangle_s=\underline{\Pi}^{\dagger}\underline{\Omega}+\underline{\Pi}^{\dagger}\underline{E}\,\underline{\Pi}+\underline{\Omega}^{\dagger}\underline{E}\langle\underline{\dot{\phi}}^{2}\rangle\underline{\Omega}\ . \tag{B1}$$

Here $\underline{E}$ denotes a diagonal matrix with elements

$$E_{\Lambda\Lambda'}=E_{Ql}\delta_{\Lambda\Lambda'} \tag{B2}$$

and E_{Ql} is the energy corresponding to ϕ_{Ql}.

The kinetic-energy correction, *term (b),* is obtained from Eqs. (2.2) and (2.5):

$$\langle\tilde{\chi}_{\Lambda}\,|\,-\nabla^2\,|\,\tilde{\chi}_{\Lambda'}\rangle_c=\Omega_c\Phi^{-}_{\Lambda}\Phi^{-}_{\Lambda'}\times\sum_{\mathbf{G}}|\,\mathbf{k}+\mathbf{G}\,|^2\times F^{*}_{\Lambda}(\mathbf{k}+\mathbf{G})F_{\Lambda'}(\mathbf{k}+\mathbf{G})\ , \tag{B3}$$

$$\langle\tilde{\chi}^{1}_{\Lambda}\,|\,-\nabla^2\,|\,\tilde{\chi}^{1}_{\Lambda'}\rangle_s=\frac{\phi^{-}_{\Lambda}}{\dot{\tilde{\phi}}^{-}_{\Lambda}}(\underline{\tilde{\Pi}}^{\dagger}\underline{\tilde{\Omega}})_{\Lambda\Lambda'}\frac{\phi^{-}_{\Lambda'}}{\dot{\tilde{\phi}}^{-}_{\Lambda'}}\ .$$

The cell integral appearing in *term (c)* is obtained from the Fourier representations of $\tilde{\chi}$ [Eq. (2.2)] and $\tilde{V}$ [Eq. (3.4)]:

$$\langle \tilde{\chi}_\Lambda \mid \tilde{V} \mid \tilde{\chi}_{\Lambda'} \rangle_c = \bar{\Phi}_\Lambda \bar{\Phi}_{\Lambda'} \sum_{\mathbf{G},\mathbf{G}'} F^*_\Lambda(\mathbf{k}+\mathbf{G}'+\mathbf{G}) \times F_{\Lambda'}(\mathbf{k}+\mathbf{G}')\tilde{V}(\mathbf{G}) \ . \quad \text{(B4)}$$

The remaining terms [(d) and the second contribution to (c)] are integrals over spheres and are obtained by inserting the one-center expansions [Eqs. (2.4) and (2.5)] into Eq. (3.7). If a one-center expansion of the potential is assumed

$$\hat{V} = \sum_{Q,L} \hat{V}_{QL} Y_L, \quad \tilde{V} = \sum_{Q,L} \tilde{V}_{QL} Y_L \quad \text{(B5)}$$

with

$$\tilde{V}_{QL}(r) = 4\pi i^l \sum_{\mathbf{G}} \tilde{V}(\mathbf{G}) j_l(Gr) Y^*_L(\hat{\mathbf{G}}) e^{i\mathbf{G}\cdot\mathbf{Q}} \Theta(s_Q - r) \ ,$$

one obtains

$$\langle \chi^1 \mid V \mid \chi^1 \rangle_s = \underline{\Pi}^\dagger \underline{I}^{11} \underline{\Pi} + \underline{\Pi}^\dagger \underline{I}^{12} \underline{\Omega} + \underline{\Omega}^\dagger \underline{I}^{21} \underline{\Pi} + \underline{\Omega}^\dagger \underline{I}^{22} \underline{\Omega} \quad \text{(B6)}$$

with

$$I^{\nu\mu}_{\Lambda\Lambda'} = \delta_{QQ'} \sum_{L''}^{L+L'} \int_0^{s_Q} \phi^{(\nu)}_{Ql}(x) V_{QL''}(x) \phi^{(\mu)}_{Ql'}(x) x^2 dx \times i^{l'-l}(-1)^{m'} C_{L,L'',-L'} \ . \quad \text{(B7)}$$

$C_{L,L',L''}$ denotes the Graunt coefficients [see Eq. (4.3)] and $-L$ is an abbreviation for $(l,-m)$. The wave functions $\phi^{(\nu)}$ are ϕ if $\nu=1$ and $\dot{\phi}$ if $\nu=2$. Because of the triangular inequality of $C_{L,L',L''}$ the L'' summation in Eq. (B7) breaks off at $L+L'$; thus, the highest angular momentum that is needed in the one-center expansion of the potential (even of $\tilde{V}$) is $L=2L_{\max}$. The application of Eqs. (B5)–(B7) to the appropriate potentials and wave functions yields explicit expressions for the considered matrix elements.

APPENDIX C: FOURIER COEFFICIENTS $\Delta(\mathbf{G})$ AND WEIGHTS d_{QL} OF THE AUXILIARY CHARGES $\Delta(\mathbf{r})$

The *weights* d_{QL} of $\Delta(\mathbf{r})$ are determined by Eqs. (4.6) and (4.7):

$$d_{QL} \int_0^{s_Q} r^{l+2} \left[1+\cos\left(\frac{\pi}{s_Q} r \right) \right] dr = M_{QL} \ , \quad \text{(C1)}$$

where M_{QL} are the moments of the local densities:

$$M_{QL} = \int_0^{s_Q} [\hat{n}^{v}_{QL}(r) + \sqrt{4\pi} n^{c,N}_Q(r)\delta_{l0}] r^{l+2} dr \ . \quad \text{(C2)}$$

With the definition

$$C_n(\pi) = \int_0^\pi x^n \cos x \, dx \quad \text{(C3)}$$

one obtains

$$d_{QL} = \frac{M_{QL}}{\left(\frac{s_Q}{\pi} \right)^{2l+3} \left(\frac{\pi^{2l+3}}{2l+3} + C_{2l+2}(\pi) \right)} \ . \quad \text{(C4)}$$

Partial integration of the rhs of Eq. (C3) leads to a recursion relation for C_n.

The *Fourier coefficients* $\Delta(\mathbf{G})$ are, by definition,

$$\Delta(\mathbf{G}) = \sum_{Q,L} \Delta_{QL}(\mathbf{G}) \quad \text{(C5)}$$

with

$$\Delta_{QL}(\mathbf{G}) = \frac{1}{\Omega_c} \int_{\Omega_c} e^{-i\mathbf{G}\cdot\mathbf{r}} \Delta_{QL}(r_Q) Y_L(\hat{\mathbf{r}}_Q) d^3r \ .$$

A one-center expansion of the exponential about the site $\mathbf{Q}$ yields the Fourier coefficients $\Delta_{QL}(\mathbf{G})$:

$$\Delta_{QL}(\mathbf{G}) = \frac{4\pi}{\Omega_c}(-i)^l S_Q^{l+3} \frac{I^C_l(Gs_Q)}{(Gs_Q)^{l+3}} d_{QL} Y_L(\hat{\mathbf{G}}) e^{-i\mathbf{G}\cdot\mathbf{Q}} \quad \text{(C6)}$$

with

$$I^C_l(\alpha) = \int_0^\alpha j_l(x) x^{l+2} \left[1+\cos\left(\frac{\pi}{\alpha} x \right) \right] dx \ . \quad \text{(C7)}$$

From the explicit form of the spherical Bessel functions $j_l(x)$, one obtains the integrals I^C_l up to $l=4$:

$$\begin{aligned} I^C_0 &= S_1 + S^C_1 \ , \\ I^C_1 &= S_1 - C_2 + S^C_1 - C^C_2 \ , \\ I^C_2 &= 3S_1 - S_3 - 3C_2 + 3S^C_1 - S^C_3 - 3C^C_2 \ , \\ I^C_3 &= 15S_1 - 6S_3 - 15C_2 + C_4 + 15S^C_1 \\ &\quad - 6S^C_3 - 15C^C_2 + C^C_4 \ , \\ I^C_4 &= 105S_1 - 45S_3 + S_5 - 105C_2 + 10C_4 \\ &\quad + 105S^C_1 - 45S^C_3 + S^C_5 - 105C^C_2 + 10C^C_4 \ , \end{aligned} \quad \text{(C8)}$$

where

$$\begin{aligned} S_n(\alpha) &= \int_0^\alpha x^n \sin x \, dx \ , \\ C_n(\alpha) &= \int_0^\alpha x^n \cos x \, dx \ , \end{aligned} \quad \text{(C9)}$$

and

$$\begin{aligned} S^C_n(\alpha) &= \int_0^\alpha x^n \sin x \cos\left(\frac{\pi}{\alpha} x \right) dx \ , \\ C^C_n(\alpha) &= \int_0^\alpha x^n \cos x \cos\left(\frac{\pi}{\alpha} x \right) dx \ . \end{aligned} \quad \text{(C10)}$$

The integrals in Eq. (C10) are determined via the recursion relations [$f = \alpha^2/(\pi^2-\alpha^2)$]

$$C^S_0 = f\left(\frac{\pi}{\alpha}\cos\alpha + \alpha \right), \quad S^C_0 = f(-\cos\alpha - 1) \ ,$$

$$S^S_0 = f\frac{\pi}{\alpha}\sin\alpha, \quad C^C_0 = f\sin\alpha \ ,$$

$$S^C_n = f\left(-\alpha^n\cos\alpha - nC^C_{n-1} - \frac{\pi}{\alpha} nS^S_{n-1} \right) ,$$

$$S^C = f\left(\alpha^n\sin\alpha - \frac{\pi}{\alpha} nC^S_{n-1} + nS^C_{n-1} \right) ,$$

$$S^S_n = f\left(\frac{\pi}{\alpha}\alpha^n\sin\alpha - nC^S_{n-1} + \frac{\pi}{\alpha} nS^C_{n-1} \right) ,$$

$$C^S = f\left(\frac{\pi}{\alpha}\alpha^n\cos\alpha + nS^S_{n-1} + \frac{\pi}{\alpha} nC^C_{n-1} \right) .$$

*Present address: Institut für Theoretische Physik, Universität des Saarlandes, D-6600 Saarbrücken, Federal Republic of Germany.

[1]*Electronic Structure, Dynamics, and Quantum Structural Properties of Condensed Matter,* edited by J. T. Devreese and P. Van Camp (Plenum, New York, 1985).

[2]G. Meissner, in *Festkörperprobleme XIII,* edited by O. Madelung and H. J. Queisser (Pergamon, Vieweg, 1973).

[3]P. Hohenberg and W. Kohn, Phys. Rev. **136**, B864 (1964).

[4]W. Kohn and L. J. Sham, Phys. Rev. **140**, A1133 (1965).

[5]O. K. Andersen, Phys. Rev. B **12**, 3060 (1975); O. K. Andersen, in *The Electronic Structure of Complex Systems,* edited by W. Temmerman and P. Phariseau (Plenum, New York, 1984).

[6]H. L. Skriver, *The LMTO Method* (Springer, Heidelberg, 1983).

[7]In contrast to calculations for solids, the LMTO calculations for molecules always use basis sets with enhanced variational freedom in the interstitial region, and it always uses the full potential; see, for example, M. Springborg and O. K. Andersen, J. Chem. Phys. (to be published), and references therein.

[8]K. H. Weyrich, Solid State Commun. **54**, 975 (1985).

[9]K. H. Weyrich and R. Siems, Z. Phys. B **61**, 63 (1985).

[10]D. Glötzel, B. Segall, and O. K. Andersen, Solid State Commun. **36**, 403 (1980).

[11]N. E. Christensen, Phys. Rev. B **29**, 5547 (1984).

[12]O. K. Andersen, Z. Pawlowska, and O. Jepsen, Phys. Rev. B **34**, 5253 (1986).

[13]K. H. Weyrich and R. Siems, Jpn. J. Appl. Phys. Suppl. **24**, 201 (1985).

[14]O. K. Andersen, H. L. Skriver, H. Nohl, and B. Johansson, Pure Appl. Chem. **52**, 93 (1979).

[15]D. R. Hamann, Phys. Rev. Lett. **42**, 662 (1979).

[16]M. T. Yin and M. L. Cohen, Phys. Rev. B **26**, 3259 (1982).

[17]M. S. Hybertsen and S. G. Louis, Phys. Rev. B **30**, 5777 (1984).

[18]O. H. Nielsen and R. M. Martin, in *Electronic Structure, Dynamics and Quantum Structural Properties of Condensed Matter,* edited by J. T. Devreese and P. Van Camp (Plenum, New York, 1985), p. 313.

[19]M. S. Methfessel (unpublished).

[20]U. von Barth and L. Hedin, J. Phys. C **5**, 1629 (1972).

[21]D. J. Chadi and M. L. Cohen, Phys. Rev. B **8**, 5747 (1973).

[22]M. A. Spackman, Acta Crystallogr., Sect. A **42**, 271 (1986).

[23]A. Svane and O. K. Andersen, Phys. Rev. B **34**, 5512 (1986).

[24]J. W. Kremer and K. H. Weyrich (unpublished).

[25]O. Jepsen, J. Madsen, and O. K. Andersen, Phys. Rev. B **26**, 2790 (1982).

[26]E. Wimmer, H. Krakauer, M. Weinert, and A. J. Freeman, Phys. Rev. B **24**, 864 (1981).

[27]K. H. Weyrich, L. Brey, and N. E. Christensen, Phys. Rev. B (to be published).

[28]K. H. Weyrich, Ferroelectrics (to be published).